



1 **Contribution of the nongrowing season to annual N₂O emissions from the**
2 **continuous permafrost region in Northeast China**

3

4 Weifeng Gao^{1,2}, Dawen Gao^{1,2,3*}, Liqian Song¹, Houcai Sheng^{4,5}, Tiji Cai^{4,5}, Hong
5 Liang^{1*}

6

7 ¹School of Environment and Energy Engineering, Beijing University of Civil
8 Engineering and Architecture, Beijing 100044, China

9 ²Center for Ecological Research, Northeast Forestry University, Harbin 150040,
10 China

11 ³State Key Laboratory of Urban Water Resource and Environment, Harbin Institute of
12 Technology, Harbin 150090, China

13 ⁴School of Forestry, Northeast Forestry University, Harbin 150040, China

14 ⁵Key Laboratory of Sustainable Forest Ecosystem Management-Ministry of Education,
15 Northeast Forestry University, Harbin 150040, China

16

17 * **Correspondence:** Dawen Gao (gaodw@hit.edu.cn); Hong Liang
18 (liangh119@hit.edu.cn)

19

20 *E-mail address:* gaowf797@nenu.edu.cn (W. Gao); gaodw@hit.edu.cn (D. Gao);

21 songliqian@nefu.edu.cn (L. Song); shenghoucai@163.com (H. Sheng);

22 caitijiu1963@163.com (T. Cai); liangh119@hit.edu.cn (H. Liang)



23 **Abstract.** Permafrost regions store large amounts of soil organic carbon and nitrogen,
24 which are major sources of greenhouse gas. With climate warming, permafrost
25 regions are thawing, releasing an abundance of greenhouse gases to the atmosphere
26 and contributing to climate warming. Numerous studies have shown the mechanism
27 of nitrous oxide (N₂O) emissions from the permafrost region during the growing
28 season. However, little is known about the temporal pattern and drivers of
29 nongrowing season N₂O emissions from the permafrost region. In this study, N₂O
30 emissions from the permafrost region were investigated from June 2016 to June 2018
31 using the static opaque chamber method. Our aims were to quantify the seasonal
32 dynamics of nongrowing season N₂O emissions and its contribution to the annual
33 budget. The results showed that the N₂O emissions ranged from -35.75 to 74.16
34 $\mu\text{g}\cdot\text{m}^{-2}\cdot\text{h}^{-1}$ during the nongrowing season in the permafrost region. The mean N₂O
35 emission from the growing season were 1.75–2.86 times greater than that of winter
36 and 1.31–1.53 times greater than that of spring thaw period due to the mean soil
37 temperature of the different specified periods. The nongrowing season N₂O emissions
38 ranged from 0.89 to 1.44 kg ha⁻¹, which contributed to 41.96–53.73% of the annual
39 budget, accounting for almost half of the annual emissions in the permafrost region.
40 The driving factors of N₂O emissions were different among during the study period,
41 growing season, and nongrowing season. The N₂O emissions from total two-year
42 observation period and nongrowing season were mainly affected by soil temperature,
43 while the N₂O emissions from growing season were controlled by soil temperature,
44 water table level, and their interactions. In conclusion, nongrowing season N₂O



45 emissions is an important component of annual emissions and cannot be ignored in
46 the permafrost region.

47

48 **1 Introduction**

49 Permafrost regions cover approximately 25% of terrestrial land and store large
50 amounts of nitrogen stocks (31–102 Pg) in soils (Harden et al., 2012). With climate
51 warming, permafrost regions are thawing and degrading globally (IPCC, 2013). Large
52 amounts of soil nitrogen have been released to the atmosphere from the permafrost
53 region. Nitrous oxide (N₂O) is a major component of N exchanged between terrestrial
54 ecosystems and atmosphere in the permafrost region and feedback to climate warming.
55 N₂O is the third most important greenhouse gas with 265 times the global warming
56 potential of CO₂ and 9 times that of CH₄, which contributes 6% to global climate
57 warming (IPCC, 2013). Soil biological processes, which release approximately 60%
58 of total natural N₂O emissions, are the largest source of N₂O emissions to the
59 atmosphere (IPCC, 2013). Permafrost regions were considered to release negligible
60 amounts of N₂O emission because of the limited mineral N content. Recently, “hot
61 spots” for N₂O emissions from permafrost regions were found in the subarctic
62 (Marushchak et al., 2011;Repo et al., 2009). The rates of N₂O emissions from bare
63 peatland could reach 31–31.4 mg m⁻² day⁻¹, which are as high as N₂O emissions from
64 tropical soil (Marushchak et al., 2011;Repo et al., 2009;Castaldi et al., 2013). The
65 cumulative N₂O emissions range from 0.9 to 1.4 g m⁻² during the growing season,
66 indicating that the permafrost region is also an important source of N₂O emissions



67 (Repo et al., 2009). In the past, research on N₂O emissions from permafrost regions
68 were mainly focused on the growing season (Repo et al., 2009;Gao et al., 2019b;Chen
69 et al., 2017). However, in the permafrost region, N₂O emissions from the nongrowing
70 season are unclear.

71

72 N₂O emissions have been widely researched during the nongrowing season in
73 different ecosystems (Maljanen et al., 2010;Merboid et al., 2013;Furon et al., 2008). A
74 significant release of N₂O emissions have been observed during the nongrowing
75 season, particularly during the spring thaw period. During the nongrowing season, the
76 rates of N₂O emission could be more than 230 g N ha⁻¹ d⁻¹ (Glenn et al., 2012;Flesch
77 et al., 2018;Chantigny et al., 2017) and the cumulative N₂O emissions released can be
78 as high as 40 kg ha⁻¹ in agricultural soil (Dunmola et al., 2010). The importance of
79 nongrowing season N₂O emissions to the annual budget, which contributed more than
80 50% of the annual values, have been shown in different ecosystems (Fu et al.,
81 2018;Virkaajarvi et al., 2010;Yanai et al., 2011). Scientists have focused primarily on
82 N₂O emissions during the nongrowing season in the agricultural (Furon et al.,
83 2008;Dietzel et al., 2011), grassland (Virkaajarvi et al., 2010;Merboid et al., 2013),
84 forest (Maljanen et al., 2010), wetland (Hao et al., 2006), and tundra ecosystems
85 (Brooks et al., 1997). Nongrowing season N₂O emissions are an essential component
86 of global N cycling. Permafrost regions, which are characterized by cold temperatures,
87 are mainly distributed in high-latitude and high-altitude areas, and are extremely
88 sensitive to climatic warming. The nongrowing season lasts for more than half of the



89 year in the permafrost region. Determining nongrowing season N₂O emissions is
90 important for accurately evaluating annual N₂O emission from permafrost regions.
91 However, N₂O emissions from permafrost regions still remain uncertain during the
92 nongrowing season.

93

94 Daxing'an Mountains, located in Heilongjiang province of Northeast China, are
95 a unique high latitude and the second largest permafrost region in China. Under the
96 threat of global warming, the permafrost region in the Daxing'an Mountains has been
97 significantly degrading and thawing (Jin et al., 2007). The area of the permafrost
98 region has decreased by 35%, leading to the deepening of the active layer, thinning of
99 the permafrost layer, and increasing ground temperatures, which changes the N cycle
100 (Jin et al., 2007). The previous in-situ N₂O measurements from permafrost region of
101 the Daxing'an Mountains have primarily been reported during the growing season or
102 the spring thaw period (Gao et al., 2019b; Cui et al., 2018; Gao et al., 2019a). In the
103 context of global climate warming, N₂O emission during the nongrowing season are
104 unclear in the permafrost region of the Daxing'an Mountains.

105

106 The typical vegetation in the permafrost region of the Daxing'an Mountains is
107 cool-temperate coniferous forest dominated by *Larix gmelinii*, forming the southern
108 boundary of the boreal forest. In this study, in-situ N₂O emission were measured from
109 the permafrost region at three forest sites in the Daxing'an Mountains for two full
110 years. The objectives of this study were to: (i) characterize the nongrowing season



111 N₂O emissions from continuous permafrost regions; (ii) evaluate the contributions
112 from the nongrowing season, particularly the spring thaw period, to annual N₂O
113 emissions; and (iii) investigations the key regulatory factors on N₂O emissions.
114 Observation of the nongrowing season N₂O emissions from permafrost regions
115 provides insight into regional climate warming and the impact of the permafrost
116 region on global climate change.

117

118 **2 Materials and Methods**

119 **2.1 Site description**

120 The experimental site was located on the continuous permafrost region in the
121 Heilongjiang Mohe Forest Ecosystem Research Station at the Daxing'an Mountains,
122 Northeast China (122°06'–122°27'E, 53°17'–53°30'N; 290–740 m elevation). The
123 study region has a typical cold temperate continental climate with a long cold winter
124 and short hot summer. Air temperature ranges from –52.3 to 36.6 °C with a mean
125 annual temperature of –4.9 °C. Mean annual precipitation is 430–550 mm, 60% of
126 which falls as rain primarily in the summer. Snow accumulation is 20–40 cm and
127 covers the land for more than half of the year (from October to April). The soil at the
128 study site is primarily brown forest soil, interspersed with meadow soil and marsh
129 soil.

130

131 The typical vegetation in this permafrost region is a temperate coniferous forest
132 with *L. gmelinii* as the dominant species. Other overstory species include *Betula*



133 *platyphylla*, *Pinus sylvestris* var. *mongolica*. Shrub species include *Ledum palustre*
134 var. *dilatatum*, *B. fruticose*, *Vaccinium uliginosum*, *V. vitis-idaea*, *Rhododendron*
135 *dauricum*, and *Alnus sibirica*. Herbaceous species include *Carex appendiculata*, *C.*
136 *schmidtii*, *Eriophorum vaginatum*, *Rubus clivicola*, and *Sanguisorba officinalis*.
137 According the water table level from low to high, three types of typical swamp forests
138 located in the permafrost region were studied: *L. gmelinii* - *Ledum palustre* var.
139 *dilatatum* swamp forest (*LL*), *L. gmelinii* - *Carex appendiculata* swamp forest (*LC*),
140 and *Betula fruticose* swamp forest (*B*). The soil physicochemical properties at the
141 three swamp forests are shown in table 1.

142

143

144

145

146

147

148

149

150

151

152

153

154



155 **Table 1.**

156 Soil properties at the three swamp forest sites in the permafrost region of Daxing'an

157 Mountains, Northeast China (mean \pm SD).

Environmental factor	<i>LL</i> site	<i>LC</i> site	<i>B</i> site
WTL	$-13.19 \pm 9.73b$	$-4.51 \pm .51a$	$0.26 \pm 5.67a$
SM _{0–10}	$117.30 \pm 14.92c$	$174.20 \pm 14.58a$	$162.31 \pm 16.14b$
SM _{10–20}	$49.54 \pm 8.28b$	$115.86 \pm 10.98a$	$115.91 \pm 9.13a$
pH _{0–10}	$4.77 \pm 0.16c$	$4.99 \pm 0.08a$	$4.89 \pm 0.11b$
pH _{10–20}	$4.93 \pm 0.18c$	$5.09 \pm 0.07a$	$4.99 \pm 0.11b$
NH ₄ ⁺ -N _{0–10}	$5.49 \pm 2.15a$	$5.98 \pm 3.03a$	$4.92 \pm 2.65a$
NH ₄ ⁺ -N _{10–20}	$3.05 \pm 1.57a$	$3.87 \pm 1.94a$	$3.43 \pm 1.88a$
NO ₃ ⁻ -N _{0–10}	$1.71 \pm 0.73a$	$1.81 \pm 1.02a$	$1.58 \pm 0.63a$
NO ₃ ⁻ -N _{10–20}	$1.29 \pm 0.57ab$	$1.44 \pm 1.02a$	$1.02 \pm 0.42b$
TOC _{0–10}	$39.95 \pm 6.91a$	$42.01 \pm 4.43a$	$35.57 \pm 5.22b$
TOC _{10–20}	$15.62 \pm 3.95b$	$18.25 \pm 2.71a$	$16.62 \pm 2.1ab$
TN _{0–10}	$2.19 \pm 0.37b$	$3.78 \pm 0.51a$	$1.97 \pm 0.69b$
TN _{10–20}	$0.83 \pm 0.15b$	$1.03 \pm 0.21a$	$0.91 \pm 0.13b$
C/N _{0–10}	$17.94 \pm 4.17a$	$11.27 \pm 144b$	$17.08 \pm 3.55a$
C/N _{10–20}	$19.26 \pm 5.65a$	$18.29 \pm 4.24a$	$18.57 \pm 3.82a$

158 WTL, water table level; SM_{0–10}, soil moisture at 0–10 cm; SM_{10–20}, soil moisture
 159 at 10–20 cm; pH_{0–10}, pH at 0–10 cm; pH_{10–20}, pH at 10–20 cm; NH₄⁺-N_{0–10},
 160 ammonium nitrogen at 0–10 cm; NH₄⁺-N_{10–20}, ammonium nitrogen at 10–20 cm;



161 NO_3^- - N_{0-10} , nitrate nitrogen at 0–10 cm; NO_3^- - N_{10-20} , nitrate nitrogen at 10–20 cm;
162 TOC_{0-10} , total organic carbon at 0–10 cm; TOC_{10-20} , total organic carbon at 10–20 cm;
163 TN_{0-10} , total nitrogen at 0–10 cm; TN_{10-20} , total nitrogen at 10–20 cm; C/N_{0-10} ,
164 carbon-to-nitrogen ratio at 0–10 cm; C/N_{10-20} , carbon-to-nitrogen ratio at 10–20 cm.

165

166 **2.2 N₂O emission measurements**

167 The field experiment was conducted from June 2016 to June 2018. Three 20 × 20
168 m plots were permanently established at each *LL*, *LC*, and *B* site, respectively. N₂O
169 emissions were measured with the static opaque chamber technique (Hutchinson et al.,
170 2000). The polypropylene chamber collar with a water-filled channel (50 cm × 50 cm
171 × 20 cm height) was randomly inserted 20 cm into the soil. Gas samples were
172 measured from 9:00 am to 11:00 am, the hours that were most representative of the
173 daily mean N₂O emissions (Alves et al., 2012). During each N₂O measurement period,
174 chambers (50 cm × 50 cm × 50 cm height) were sealed by filling the collars with
175 water and used to collect N₂O from the soil. Four-chamber headspace air samples
176 were taken using a 50-mL plastic syringe at 0, 15, 30, and 45 min after chamber
177 closure (Liu et al., 2019). Samples were injected into pre-evacuated 100 mL gas
178 sampling bags (Delin Gas Packing Co., Dalian, China) for subsequent laboratory
179 analysis. The air temperature inside the chamber was recorded when gas samples were
180 being retrieved. Gas samples were taken twice per month during the growing season
181 from June to September, monthly during the winter from October to December, and
182 every three to ten days during the spring thaw period from March to May (45



183 sampling events in total).

184

185 The gas N₂O concentration was analyzed with a gas chromatograph coupled with
186 an electron capture detector (ECD) (Shimadzu GC2010, Shimadzu Analytical and
187 Measuring Instruments Division, Kyoto, Japan). Compressed air containing 0.378
188 ppm N₂O was used for calibration. N₂ was used as the carrier gas with a flow rate of
189 20 mL min⁻¹. The N₂O was separated using a 1-m stainless steel column with an inner
190 diameter of 2 mm from Porapak Q (80/100 mesh), and was detected by an ECD. The
191 temperature for gas separation was maintained at 70 °C and the detector was set at
192 250 °C.

193

194 **2.3 Measurements of meteorological and soil physiochemical properties**

195 Soil temperature (ST) at 5, 10, and 15 cm deep was monitored at each collar
196 using a portable digital thermometer with a thermocouple probe (JM-624, Jinming
197 Corp., Tianjin, China). During the growing season, the water table level (WTL) was
198 measured near the chamber in each plot using a ruler (Dobbie and Smith, 2006). In
199 the nongrowing season, soil moisture was determined by the oven-drying method.

200

201 Using a 3.8 cm diameter stainless-steel sampling probe, soil samples were taken
202 from the upper 0–10 cm and lower 10–20 cm soil layers close to each collar. Fine
203 roots and visible organic debris were removed by passing the soil samples through a
204 2-mm sieve. Then, samples were stored in an insulated box (Esky) and stored at 4 °C



205 for subsequent chemical analysis.

206

207 Soil moisture contents were determined by drying at 105 °C for 48 h followed by
208 calculating the weight loss. Soil samples were air dried and sieved to <2 mm
209 aggregate size and used to measure the soil pH. Soil pH was measured in a 2:5
210 air-dried soil: deionized water mixture using an InoLab pH meter (WTW InoLab pH
211 730, Weilheim, Germany). Soil mineral N, ammonium ($\text{NH}_4^+\text{-N}$), and nitrate ($\text{NO}_3^-\text{-N}$)
212 content were determined on 10 g samples of fresh soil based on a 1 mol/L KCl
213 solution extraction procedure. The extracts were filtered through a 0.45 μm
214 pore-diameter syringe filter, and then soil mineral N was analyzed using a Lachat
215 flow-injection auto-analyzer (Seal Analytical AA3, Norderstedt, Germany). For the
216 analyses of total N and C, sub-samples were further ground to a fine powder (<0.15
217 mm). Total N concentration was measured on aliquots of 1.0 g of soil using
218 semi-micro-Kjeldahl method. The TOC content was determined by oxidation at
219 170 °C, with potassium dichromate in the presence of sulfuric acid. The excess
220 potassium dichromate was titrated with a solution of Mohr's salt.

221

222 **2.4 Statistical analysis**

223 The N_2O emissions were calculated as reported by (Hou et al., 2012). A positive
224 regression indicates the emission from soil to the atmosphere. A negative regression
225 indicates a net uptake by the soil from the atmosphere. Cumulative N_2O emissions
226 were linearly and sequentially accumulated from the emissions between every two



227 adjacent intervals of the measurements following the procedure described by Ding et
228 al. (2007).

229

230 The calendar year was divided into three seasons: winter, spring thaw period, and
231 growing season. The winter was defined as the period during which the daily mean air
232 temperature remained below 0 °C for at least five consecutive days. The spring thaw
233 period was defined as the period when the daily maximum air temperature exceeded
234 0 °C and ended at soil thawing to a depth of 20 cm. The growing season was defined
235 as the period that lasts from the end of the spring thaw period to the beginning of
236 winter. We designated the winter and spring thaw period as the nongrowing season.

237

238 A one-way analysis of variance was used to test the difference of N₂O emissions
239 and environment factors in the three swamp forest sites. A T-test was used to identify
240 the differences in N₂O emissions between 2016/2017 and 2017/2018. The correlations
241 between the N₂O emissions and environmental factors were tested using Pearson's
242 correlation analysis. A linear correlation analysis and multivariate regression analysis
243 were conducted to create explanatory models using the same variables as those used
244 for describing the temporal variation of N₂O emissions. R software (Version 3.4.1,
245 <https://www.r-project.org/>) was used for the statistical analyses. Significance was
246 analyzed using Fisher's least significant difference (LSD) test at a probability level of
247 95% ($P < 0.05$). All figures were drawn using OriginPro 2018 software (OriginLab
248 Corp., Northampton, MA, U.S.A.).

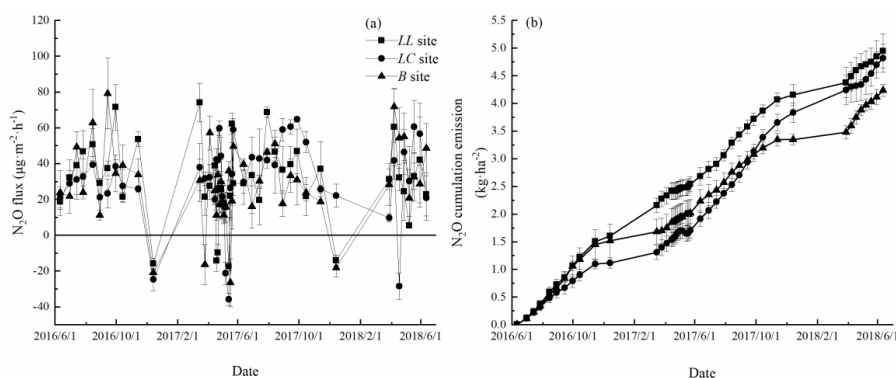


249

250 3 Results

251 3.1 Temporal variation of N₂O emissions

252 During the two-year observation period, there was significant temporal variation
253 in N₂O emissions in the permafrost region of the Daxing'an Mountains (Fig. 1a).
254 However, the temporal pattern of N₂O emissions were different in the three swamp
255 forests. The N₂O emissions ranged from -17.40 to 74.16, -35.75 to 64.73, and -26.47
256 to 79.25 $\mu\text{g}\cdot\text{m}^{-2}\cdot\text{h}^{-1}$ in the *LL*, *LC*, and *B* sites, respectively (Fig. 1a). The highest N₂O
257 emissions occurred in different periods in three swamp forests, namely, they occurred
258 in the beginning of the spring thaw period in the *LL* site and at the end of growing
259 season in the *LC* and *B* sites. The lowest N₂O emissions from the three swamp forest
260 sites were all observed in the spring thaw period. Negative emissions mainly occurred
261 during the winter and spring thaw period. The N₂O emissions during the nongrowing
262 season mainly ranged from -17.40 to 74.16, -35.75 to 60.76, and -26.47 to 71.82
263 $\mu\text{g}\cdot\text{m}^{-2}\cdot\text{h}^{-1}$ in the *LL*, *LC*, and *B* sites, respectively.



264

265 **Figure 1.** N₂O emissions (A) and cumulative N₂O emissions (B) from three types of



266 swamp forests in the permafrost region of the Daxing'an Mountains, Northeast China

267

268 The annual mean N₂O emissions ranged from 27.80 to 32.51, 26.10 to 37.89, and
269 25.86 to 33.16 $\mu\text{g}\cdot\text{m}^{-2}\cdot\text{h}^{-1}$ in the *LL*, *LC*, and *B* sites, respectively (Table 2). The mean
270 N₂O emissions from the growing season typically higher than that of winter and the
271 spring thaw period in the three swamp forest sites. In 2016/2017, the mean N₂O
272 emissions were all highest in the growing season and lowest in the winter. In contrast,
273 during 2017/2018, the mean N₂O emissions were lowest during the spring thaw
274 period in the *LC* site and highest during the spring thaw period in the *B* site. For the
275 different types of swamp forests, the mean N₂O emissions from the *LC* site were
276 significantly higher than the mean N₂O emissions in the *B* site in the 2017/2018
277 growing season. There was no significant difference in N₂O emissions during the
278 winter, spring thaw period, and annually in the three swamp forests. The N₂O
279 emissions from different periods were generally not significantly different between
280 the two years. Differences in N₂O emissions were found during the growing season
281 and spring thaw period. The mean N₂O emissions during the growing season from the
282 *LC* site and the N₂O emissions during the spring thaw period from the *B* site were
283 both significantly higher in 2017/2018 than 2016/2017.

284



285 **Table 2.**
 286 Summary of N₂O emissions during specified periods from the three swamp forest sites in the permafrost region of the Daxing'an Mountains,
 287 Northeast China

Specified period	Duration		Mean N ₂ O emissions ($\mu\text{g}\cdot\text{m}^{-2}\cdot\text{h}^{-1}$)					
	(Days)		2016/2017			2017/2018		
	2016/2017	2017/2018	LL site	LC site	B site	LL site	LC site	B site
Growing season	134	129	40.42 ± 15.97Aa	29.54 ± 7.30Ab	38.35 ± 23.42Aa	40.09 ± 14.68ABa	47.73 ± 12.27Aa	33.17 ± 12.48Ba
Nongrowing season								
Winter	155	161	19.80 ± 34.74Aa	9.62 ± 29.69Aa	17.41 ± 33.14Aa	14.95 ± 26.23Aa	33.31 ± 16.25Aa	8.13 ± 22.89Aa
Spring thaw period	77	75	22.49 ± 24.90Aa	27.56 ± 26.06Aa	20.89 ± 21.73Ab	32.74 ± 16.69Aa	31.04 ± 31.31Aa	41.66 ± 18.78Aa
Annual	366	365	27.80 ± 24.36Aa	26.10 ± 22.44Aa	25.86 ± 24.06Aa	32.51 ± 18.31Aa	37.89 ± 22.26Aa	33.16 ± 19.55Aa

288 The different capital letters indicate that the N₂O emissions were significantly different among the types of swamp forest; different lowercase
 289 letters indicate that the N₂O emissions were significantly different between the two years.



290 **3.2 Seasonal contribution of N₂O emissions to the annual budget**

291 Cumulative N₂O emissions primarily increased during the study period (Fig. 1b).
292 The annual N₂O emissions ranged from 2.27 to 2.68, 1.92 to 2.90, and 2.00 to 2.24 kg
293 ha⁻¹ yr⁻¹ in the *LL*, *LC*, and *B* sites, respectively (Table 3). The cumulative N₂O
294 emissions during the growing season ranged from 1.02 to 1.46 kg ha⁻¹, which
295 contributed to 46.27 to 58.04% to the annual emissions. The cumulative N₂O
296 emissions from the growing season were higher than the cumulative N₂O emissions
297 during the winter and spring thaw periods, and were 1.2 to 3.2 times greater than that
298 of the winter and 1.5 to 3.7 times greater than that of the spring thaw period. The
299 cumulative N₂O emissions during the nongrowing season were mainly lower than
300 during the growing season, which contributed to 41.96–53.73% to annual emissions.
301 The cumulative N₂O emissions during the spring thaw period ranged from 0.35 to
302 0.66 kg ha⁻¹, contributing to 15.63 to 33.00% to the annual emissions.

303



304 **Table 3.**

305 The cumulative N₂O emissions and its contribution to annual N₂O emissions from the three swamp forest sites in the permafrost region of
 306 Daxing'an Mountains, Northeast China.

Forest types	Year	Cumulative N ₂ O emissions (kg ha ⁻¹)				Contribution to annual N ₂ O emissions (%)				
		Annual	GS	NGS	Winter	STP	GS	NGS	Winter	STP
<i>LL</i> site	2016/2017	2.68 ± 0.15	1.24 ± 0.06	1.44 ± 0.21	1.00 ± 0.20	0.44 ± 0.04	46.27	53.73	37.31	16.42
	2017/2018	2.27 ± 0.16	1.21 ± 0.07	1.06 ± 0.18	0.56 ± 0.16	0.50 ± 0.03	53.30	46.70	24.67	22.03
<i>LC</i> site	2016/2017	1.92 ± 0.14	1.03 ± 0.13	0.89 ± 0.13	0.48 ± 0.11	0.41 ± 0.02	53.65	46.35	25.00	21.35
	2017/2018	2.90 ± 0.11	1.46 ± 0.03	1.44 ± 0.10	0.93 ± 0.12	0.51 ± 0.03	50.34	49.66	32.07	17.59
<i>B</i> site	2016/2017	2.24 ± 0.21	1.30 ± 0.15	0.94 ± 0.08	0.58 ± 0.07	0.35 ± 0.01	58.04	41.96	25.89	15.63
	2017/2018	2.00 ± 0.22	1.02 ± 0.11	0.98 ± 0.22	0.32 ± 0.20	0.66 ± 0.08	51.00	49.00	16.00	33.00

307 GS: growing season; NGS: nongrowing season; STP: spring thaw period.

308



309 3.3 Temporal control of soil N₂O emissions

310 The relationship between N₂O emissions and environmental factors during the
311 different specified periods are shown in Table 4. During the entire two-year
312 observation period, the N₂O emission were all significantly positively correlated with
313 soil temperature at 5, 10, and 15 cm in the three swamp forest sites. Except for the soil
314 temperature, the N₂O emissions from the *LL* site were also positively correlated with
315 air temperature ($P < 0.05$) and C/N_{0-10} ($P < 0.05$) and negatively correlated with pH_{0-10}
316 ($P < 0.01$), pH_{10-20} ($P < 0.05$), $NO_3^- - N_{0-10}$ ($P < 0.05$), $NO_3^- - N_{10-20}$ ($P < 0.05$), and TN_{0-10}
317 ($P < 0.05$). The N₂O emissions from the *LC* site were significantly positively correlated
318 with TOC_{0-10} ($P < 0.01$) and TN_{10-20} ($P < 0.01$). The N₂O emissions from the *B* site were
319 significantly positively correlated with air temperature ($P < 0.001$), $NH_4^+ - N_{0-10}$
320 ($P < 0.05$), and $NH_4^+ - N_{10-20}$ ($P < 0.05$). Similar to the entire period, the N₂O emissions
321 from the nongrowing season were mainly significantly positively correlated with soil
322 temperature in the *LC* and *B* sites and weakly positively correlated with soil
323 temperature in the *LL* sites. The N₂O emissions from the *LL* site were also
324 significantly negatively correlated with pH_{0-10} ($P < 0.05$) and TN_{0-10} ($P < 0.001$); the
325 N₂O emissions from the *LC* site were significantly positively correlated with TN_{0-10}
326 ($P < 0.05$). The N₂O emissions from the *B* site were significantly positively correlated
327 with air temperature ($P < 0.05$), $NH_4^+ - N_{0-10}$ ($P < 0.01$), $NH_4^+ - N_{10-20}$ ($P < 0.01$), and
328 $NO_3^- - N_{0-10}$ ($P < 0.05$). For the growing season, the impact of environmental factors on
329 N₂O emissions were complicated. The N₂O emissions were significantly positively
330 correlated with T_{15} ($P < 0.05$) and negatively correlated with $NO_3^- - N_{0-10}$ ($P < 0.05$) and



331 NO_3^- - N_{10-20} ($P < 0.01$) in the *LL* site. The N_2O emissions from *LC* site were
332 significantly influenced by air temperature, water table level, NO_3^- -N, TOC, TN, and
333 C/N ratio. The N_2O emissions from the *B* site were only significantly positively
334 correlated with water table level ($P < 0.05$).



335 **Table 4.**
 336 The relationship between N₂O emissions and environmental factors from three swamp forest sites in the permafrost region of the Daxing'an
 337 Mountains, Northeast China.

Environmental factor	Two full-year			Growing season			Nongrowing season		
	LL site	LC site	B site	LL site	LC site	B site	LL site	LC site	B site
<i>T_a</i>	0.17*	0.14	0.30***	-0.26 ⁺	-0.50***	0.15	0.11	0.16	0.26*
<i>T₅</i>	0.33***	0.26**	0.35***	0.07	-0.13	0.19	0.17	0.25*	0.29**
<i>T₁₀</i>	0.37***	0.28**	0.36***	0.20	-0.03	0.21	0.20 ⁺	0.26*	0.31**
<i>T₁₅</i>	0.39***	0.30***	0.34***	0.30*	0.06	0.14	0.21 ⁺	0.32**	0.32**
WTL				-0.13	-0.29*	0.29*			
SM ₀₋₁₀							-0.08	-0.02	0.03
SM ₁₀₋₂₀							-0.10	0.08	-0.03
pH ₀₋₁₀	-0.24**	0.07	-0.18 ⁺	-0.01	0.08	-0.20	-0.25*	0.08	-0.15



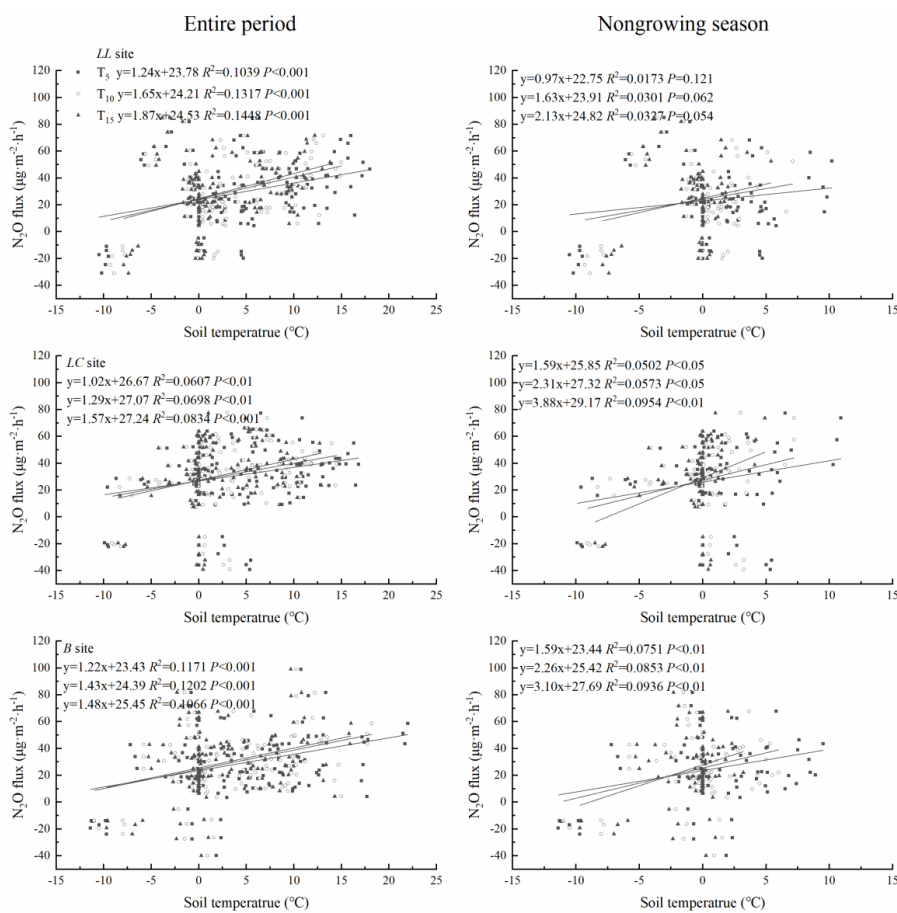
pH ₁₀₋₂₀	-0.21*	0.15	-0.12	-0.05	0.14	0.05	-0.17	0.22 ⁺	-0.19
NH ₄ ⁺ -N ₀₋₁₀	0.08	0.05	0.20*	0.21	0.19	-0.06	0.07	-0.11	0.32**
NH ₄ ⁺ -N ₁₀₋₂₀	0.05	0.01	0.24*	-0.08	-0.23	0.14	0.21 ⁺	0.15	0.34**
NO ₃ ⁻ -N ₀₋₁₀	-0.24*	0.05	0.01	-0.32*	0.28*	-0.16	-0.08	0.09	0.29*
NO ₃ ⁻ -N ₁₀₋₂₀	-0.22*	0.09	-0.11	-0.36**	0.36*	-0.02	0.01	0.11	0.03
TOC ₀₋₁₀	0.13	0.26**	-0.14	0.23	0.48***	-0.15	-0.16	0.01	-0.05
TOC ₁₀₋₂₀	0.08	0.10	-0.06	0.03	-0.02	-0.01	-0.14	0.11	-0.09
TN ₀₋₁₀	-0.21*	0.06	-0.03	0.08	-0.35*	-0.04	-0.43***	0.14	0.03
TN ₁₀₋₂₀	0.01	0.26**	-0.16 ⁺	0.19	0.65***	-0.16	-0.06	0.26*	-0.15
C/N ₀₋₁₀	0.21*	0.15	-0.08	0.13	0.53***	-0.05	0.10	-0.17	-0.14
C/N ₁₀₋₂₀	0.06	-0.14	0.04	-0.18	-0.54***	0.04	-0.13	-0.13	0.05

338 ⁺: indicates significant effects at $P < 0.1$; *: indicates significant effects at $P < 0.05$; **: indicates significant effects at $P < 0.01$; ***: indicates significant effects at $P < 0.001$.

339 indicates significant effects at $P < 0.001$.



340 The Pearson correlation analysis showed that the soil temperature was the key
341 environmental factor controlling the N₂O emissions during the entire observation
342 period and the nongrowing season. During the entire observation period, soil
343 temperature at 5, 10, and 15 cm could explain 10.39 to 14.48, 6.07 to 8.34, and 10.66
344 to 12.02% of the temporal variation of N₂O emissions in the *LL*, *LC*, and *B* sites,
345 respectively. During the nongrowing season, N₂O emissions from the *LL* site were
346 weakly positively correlated with soil temperature, explaining 1.73 to 3.27% of N₂O
347 emissions. The soil temperature could explain 5.02 to 9.54% and 7.51 to 9.36% of the
348 N₂O fluctuation in the *LC* and *BC* sites, which were lower than the entire observation
349 period.
350



351

352 **Figure 2.** The linear models between N₂O emissions and soil temperature during the
353 entire observation period and nongrowing season in the three swamp forest sites in the
354 permafrost region of the Daxing'an Mountains, Northeast China.

355

356 During the growing season, multivariate regression analyses showed that the
357 N₂O emissions were affected by soil temperature, water table level, and their
358 interactions (Table 5). Soil temperature, water table level, and their interactions could
359 explain 26.35, 19.46, and 12.36% of the temporal variation of N₂O emissions in the
360 three swamp forest sites, respectively.



361

362 **Table 5.**

363 Models of N₂O emissions during the growing season against soil temperature and
364 water table level for the three swamp forest sites in the permafrost region of the
365 Daxing'an Mountains, northeast China.

Forest type	a	b	c	d	R ²	P
<i>LL</i> site	-11.55	4.03	-3.19	0.25	0.2635	<0.001
<i>LC</i> site	22.44	0.94	-3.99	0.28	0.1946	<0.01
<i>B</i> site	27.57	0.77	-1.50	0.21	0.1236	<0.05

366 The regression models are: $y = a + b \times T_5 + c \times \text{WTL} + d \times T_5 \times \text{WTL}$, where a, b, c, and d
367 are the regression coefficients.

368

369 **4 Discussion**

370 **4.1 Soil temperature controls the mean N₂O emissions from the different periods**

371 In previous studies, the N₂O emissions from the permafrost region primarily
372 focused on emissions during the growing season (Gil et al., 2017; Lamb et al.,
373 2011; Voigt et al., 2017). Permafrost regions are mainly distributed in high-altitude and
374 high-latitude zones. It was difficult to measure N₂O emissions during the nongrowing
375 season in the cold climate conditions of the permafrost region. Publications on
376 nongrowing season N₂O emissions are scarce and the difference of mean N₂O
377 emissions among the winter, spring thaw period, and growing season are unknown in
378 the permafrost region.



379

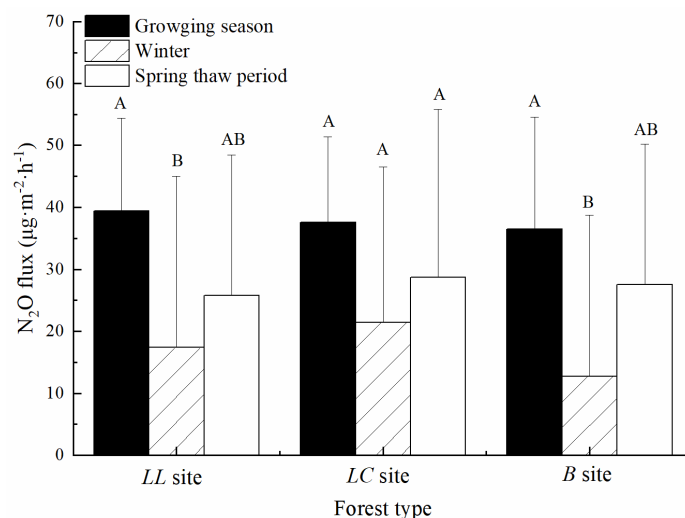
380 The nongrowing season N₂O emission ranged from -35.75 to $74.16 \mu\text{g}\cdot\text{m}^{-2}\cdot\text{h}^{-1}$
381 in the permafrost region of the Daxing'an Mountains, northeast China. The results
382 were similar to the rate of annual N₂O emission (-35.75 to $79.25 \mu\text{g}\cdot\text{m}^{-2}\cdot\text{h}^{-1}$) in the
383 permafrost region of the Daxing'an Mountains and within the range of N₂O emissions
384 reported in permafrost ecosystems (-35.75 to $2662 \mu\text{g}\cdot\text{m}^{-2}\cdot\text{h}^{-1}$) (Gao et al., 2019a; Mu
385 et al., 2017). The N₂O emissions confirmed our previous findings that the N₂O
386 emissions from the Daxing'an Mountains ranged within the intermediate range for
387 permafrost ecosystems (Gao et al., 2019b).

388

389 The annual N₂O emissions showed significant temporal variations in grasslands
390 (Du et al., 2006). There were significant differences in the mean N₂O emissions in the
391 spring, summer, autumn, and winter in grasslands, whereas the temporal pattern over
392 the course of the five-year study (Du et al., 2006). The N₂O was taken up during the
393 freezing period and emitted during the thawing period and growing season in marshes,
394 indicating that the emissions were different among the three specified periods (Hao et
395 al., 2006). These trends were also observed in the permafrost region. In the “hot spots”
396 of N₂O emission from permafrost region, high N₂O emissions were observed during
397 the nongrowing season in the bare peatland, which contributed 20–69% to the annual
398 emissions from the bare peatland (Marushchak et al., 2011). In the vegetated
399 permafrost ecosystem, the N₂O emissions during the nongrowing season, growing
400 season, and annually were mainly negligible (Marushchak et al., 2011). The N₂O



401 emissions from the spring thaw period and nongrowing season were lower than that of
402 growing season in the permafrost region of the Daxing'an Mountains (Chen et al.,
403 2017;Gao et al., 2019a;Wu et al., 2019). However, the drivers of N₂O emissions
404 between the nongrowing season and growing season were not clear in the permafrost
405 region. Our results showed that the N₂O emissions were the highest during the
406 growing season and lowest during the nongrowing season. The mean N₂O emissions
407 from the growing season were significantly higher than the emissions from the winter
408 in the *LL* and *B* sites, whereas the N₂O emissions during the spring thaw period was
409 not significantly different from growing season and winter in the three swamp forests
410 (Fig. 3). The N₂O emissions from the growing season were 1.75–2.86 times greater
411 than the winter emissions and 1.31–1.53 times greater than during the spring thaw
412 period in the three forest types.



413
414 **Figure 3.** The difference of N₂O emissions among the growing season, winter, and
415 spring thaw period in the permafrost region of the Daxing'an Mountains, Northeast



416 China.

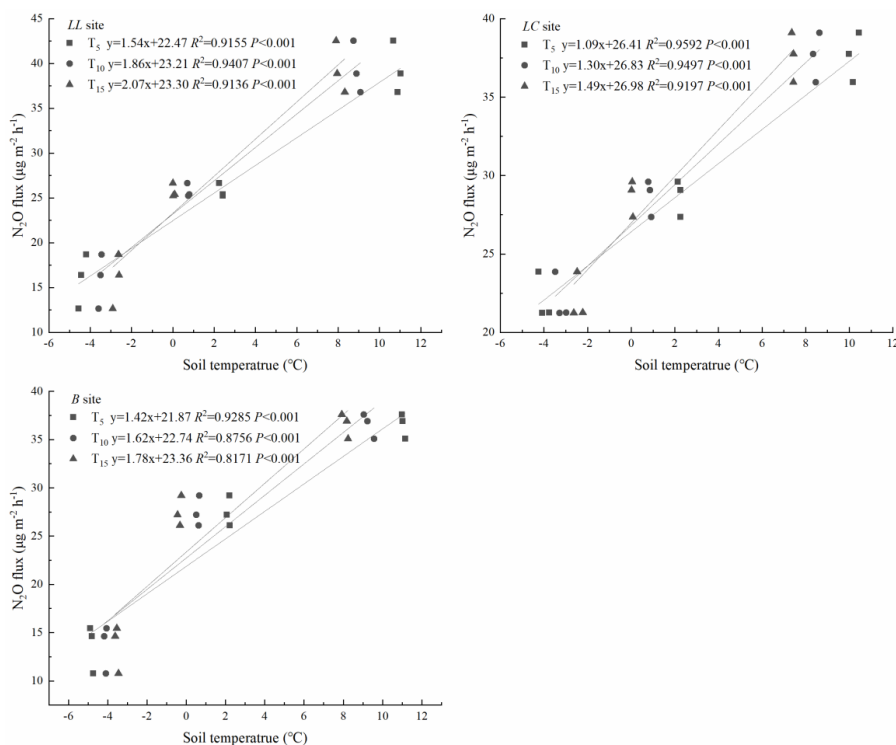
417

418 We found that the mean N₂O emissions of the three specified periods were
419 significantly positively correlated with soil temperature at 5, 10, and 15 cm, which
420 could explain 91.36–94.07, 91.97–95.92, and 81.71–92.85% of the temporal variation
421 of mean N₂O emissions in the *LL*, *LC*, and *B* sites, respectively (Fig. 4). In a
422 laboratory experiment, the N₂O emissions were strongly dependent on soil
423 temperatures above zero (Oquist et al., 2004). The net N₂O production rates at –4 °C
424 equaled those observed at +10 to +15 °C in the boreal forest soil (Oquist et al., 2004).
425 However, the field soil temperature in the winter in the Daxing’an Mountains was
426 significantly lower than the simulated cold temperature in the laboratory, meaning that
427 the winter N₂O emissions may be lower than N₂O emissions during the growing
428 season (Oquist et al., 2004). In the nongrowing season, soil moisture was consistently
429 saturated in the 0–10 cm soil layer of three swamp forests, which implies that N₂O
430 production occurred predominantly due to denitrification. The denitrification rates
431 showed similar temporal variations of N₂O emissions in agricultural soil in the winter
432 (Tatti et al., 2014). The copy numbers of denitrifier genes (*nirS* and *nirK*) remained
433 stable from November to January and increased in March and April, indicating that
434 N₂O emissions during the spring thaw period were higher than during the winter (Tatti
435 et al., 2014). During the growing season, N₂O emissions were significantly positively
436 correlated with soil temperature in the permafrost region (Marushchak et al., 2011; Cui
437 et al., 2018; Chen et al., 2017). Thus, the soil temperature controlled the mean N₂O



438 emissions during the winter, spring thaw period, and growing season. Soil
439 temperature was the key environmental factor determining the temporal variation of
440 N₂O emissions in the permafrost region of the Daxing'an Mountains.

441



442

443 **Figure 4.** The relationship between mean N₂O emission from different specified
444 periods and soil temperature in the permafrost region of the Daxing'an Mountains,
445 Northeast China.

446

447 4.2 Contribution of nongrowing season to annual N₂O budget

448 The cumulative N₂O emissions from the permafrost region was mainly evaluated
449 during the growing season (Repo et al., 2009; Takakai et al., 2008; Gao et al., 2019b).



450 The N₂O emissions from the permafrost region were as high as 14 kg ha⁻¹ and
451 released approximately 0.1 Tg yr⁻¹ N₂O emissions to the atmosphere in the bare peat
452 region of the Arctic, accounting for up to 0.6% of the global annual N₂O emissions
453 (Repo et al., 2009). A few studies have indicated that the nongrowing season
454 contributed greatly to the annual N₂O emissions from the frigid terrestrial ecosystems
455 (Li et al., 2012;Zhang et al., 2018;Fu et al., 2018). However, the contribution of the
456 nongrowing season to the annual N₂O budget is uncertain in the permafrost region.

457

458 The cumulative N₂O emissions during the nongrowing season ranged from 0.89
459 to 1.44 kg ha⁻¹, which contributed to 41.96–53.73% of the annual budget in the
460 permafrost region of the Daxing'an Mountains. In frigid terrestrial ecosystems, the
461 N₂O emissions of the nongrowing season contributed to 20–74% of the annual
462 emissions; therefore, our results were within the range of previous studies (Li et al.,
463 2012;Zhang et al., 2018;Fu et al., 2018;Marushchak et al., 2011). During the spring
464 thaw period, the soil temperature and soil moisture dramatically changed, which
465 significantly affected the release of N₂O emissions. A pulse or burst of N₂O emissions
466 have been observed in agriculture (Flesch et al., 2018), grassland (Virkajärvi et al.,
467 2010), forest (Wu et al., 2010), marsh (Song et al., 2008), and peat ecosystems (Flesch
468 et al., 2018). The pulse N₂O emissions during the spring thaw period had enormous
469 influence on the contribution of the nongrowing season to the annual budget in the
470 frigid terrestrial ecosystems (Li et al., 2012;Fu et al., 2018). When the pulse of N₂O
471 emissions occurred during the spring thaw period, emissions from the non-growing



472 seasons dominated (67–74%) the annual total emissions (Fu et al., 2018). When no
473 pulse of N₂O emissions were found during the spring thaw period, the contribution of
474 the spring thaw period to the total annual N₂O budget was very small and accounted
475 for only 6.6% of the annual emissions (Li et al., 2012). In the present study, there was
476 no significant large burst of N₂O emissions during the spring thaw period. The
477 cumulative N₂O emissions during the spring thaw period ranged from 0.35 to 0.66 kg
478 ha⁻¹ and contributed 15.61 to 33.00% of the annual budget in the permafrost region of
479 the Daxing’an Mountains, and these ranges were generally lower than the emissions
480 during the winter and growing season.

481

482 The mean N₂O emissions were the lowest in the winter and highest in the
483 growing season, which were not the same as the cumulative N₂O emissions in the
484 three swamp forests. The permafrost region of the Daxing’an Mountains was located
485 at a high latitude, which had a longer nongrowing season than growing season. In the
486 permafrost region of the subarctic, the nongrowing season lasts for more than 9
487 months (283 days) (Marushchak et al., 2011). The length of winter was more than
488 twice of spring thaw spring in the Daxing’an mountains. Although the mean N₂O
489 emissions in winter were lower than during spring thaw period, the cumulative N₂O
490 emissions in winter were higher than the emissions from the spring thaw period. The
491 cumulative N₂O emissions during winter were as important as the spring thaw period.
492 Only one study reported the cumulative N₂O emissions during nongrowing seasons in
493 the permafrost region. Marushchak et al. (2011) found that the N₂O emissions from



494 the nongrowing season contributed 20–69% to the annual emissions in the bare peat
495 zone of the permafrost region. Our results confirmed that half of the N₂O emissions
496 were released during the nongrowing season, indicating that the N₂O emissions during
497 the nongrowing season cannot be ignored in the permafrost regions. In the future, the
498 N₂O emissions of the nongrowing season should be emphasized in the permafrost
499 region, especially in the context of global climate change.

500

501 **4.3 Drivers of N₂O emissions on different temporal scales**

502 Most previous studies on the permafrost region have focused exclusively on the
503 growing season (Gao et al., 2019b; Repo et al., 2009; Cui et al., 2018). The N₂O
504 emissions during the growing season were mainly influenced by air temperature, soil
505 temperature, water table level, soil moisture, precipitation, pH, NH₄⁺-N, NO₃⁻-N,
506 TOC, gross N mineralization, N content, and C/N ratio in the permafrost region (Ma
507 et al., 2007; Gil et al., 2017; Marushchak et al., 2011; Chen et al., 2017; Cui et al.,
508 2018; Paré and Bedard-Haughn, 2012). However, the drivers of nongrowing season
509 N₂O emission remain unknown in the permafrost region.

510

511 N₂O production processes are very complex and can be produced by nitrification,
512 nitrifier denitrification, and denitrification in the permafrost region (Ma et al.,
513 2007; Gil et al., 2017; Siljanen et al., 2019). Soil water content controls the redox
514 conditions in the soil, which determines the pathway of N₂O emissions. The soil water
515 content showed significant temporal variation in the permafrost region of the



516 Daxing'an Mountains. Thus, the pathway of N₂O emissions may be different in the
517 nongrowing season and growing season. During the growing season, the water table
518 level ranged from -31.6 to 10.27 cm in the three swamp forests. N₂O emission may
519 have come from simultaneous nitrification and denitrification in the *LL* site and
520 denitrification in the *LC* and *BC* sites (Gao et al., 2019b). In the 2016 growing season,
521 the N₂O emissions mainly controlled multiple environmental factors (Gao et al.,
522 2019b). Our results show that the N₂O emissions were driven by soil temperature and
523 water table level and their interactions, explaining 12.36–26.35% of temporal
524 variation of N₂O emissions during the two growing seasons. As the permafrost
525 ecosystem is strongly temperature limited, the N₂O emissions were mainly
526 significantly positively correlated with soil temperature in the permafrost region
527 (Marushchak et al., 2011; Cui et al., 2018; Chen et al., 2017). Soil temperature could
528 increase nitrification and denitrification, thus promoting the release of N₂O flux. Wu
529 et al. (2019) found that the N₂O emissions were significantly negatively correlated
530 with soil moisture in the three forests of the Daxing'an Mountains. Our results
531 confirm that the decrease of the water table level was beneficial to the release of N₂O
532 emissions. Soil temperature and water table level were key factors controlling the
533 emission of N₂O during the growing season. In contrast, the nongrowing season N₂O
534 emissions were mainly controlled by soil temperature in the permafrost region of the
535 Daxing'an Mountains.

536

537 During the nongrowing season, the soil moisture was consistently exceeded 60%



538 in the three swamp forests. The N₂O emissions were major produced by
539 denitrification in the permafrost region. The nongrowing season N₂O emissions were
540 positively correlated with soil temperature in the three swamp forests. The denitrifier
541 genes were stable during the winter and increased during the spring thaw period (Tatti
542 et al., 2014). Wertz et al. (2013) found that the community structures of denitrifiers
543 were different between below-zero and above-zero temperatures. During the
544 nongrowing season, the soil temperature affected the abundance and community
545 structures of denitrifiers and thus the release of N₂O emissions in the permafrost
546 region of the Daxing'an Mountains. In the field, environmental factors are always
547 changing; therefore, any factor can be a limiting factor for a long period. The N₂O
548 emissions from the two-year study period were controlled by soil temperature in the
549 permafrost region of the Daxing'an Mountains. Soil temperature was the major
550 limiting factor related to annual N₂O emissions in the permafrost region. Except for
551 soil temperature, the N₂O emissions from the permafrost region were also affected by
552 pH, NO₃⁻-N, TN, and C/N ratio.

553

554 **5 Conclusions**

555 The N₂O emissions from the nongrowing season were quantified in the
556 permafrost region. The N₂O emissions ranged from -35.75 to 74.16 μg·m⁻²·h⁻¹
557 during the nongrowing season. The mean N₂O emissions were lowest in the winter
558 and highest in the growing season, and were controlled by soil temperature. The
559 cumulative N₂O emissions during the nongrowing season greatly contributed to the



560 annual budget, which cannot be ignored. In the different periods studied, N₂O
561 emissions had different key limiting factors in the permafrost region. The nongrowing
562 season and the annual N₂O emissions were driven by soil temperature, whereas the
563 growing season N₂O emissions were affected by soil temperature, water table level,
564 and their interaction.

565

566 *Data availability.* The data used in the present study are available in the Supplement.

567

568 *Supplement.* The supplement related to this article is available online at:

569 <https://doi.org/>

570

571 *Author contributions.* Dawen Gao and Hong Liang designed and guided the
572 experiment, provided supervision, and contributed to revise of the manuscript. Tijiu
573 Cai and Houcai Sheng provided and set up field experimental sites. Liquan Song
574 conducted laboratory analysis. Weifeng Gao conducted the field sampling, analyzed
575 the data and wrote the manuscript.

576

577 *Competing interests.* The authors declare that they have no conflict of interest.

578

579 *Acknowledgements.* We are sincerely grateful to Heilongjiang Mohe Forest Ecosystem
580 Research Station.

581



582 *Financial support.* This work was supported by the National Natural Science
583 Foundation of China (No. 31870471, 31971468).

584

585 *Review statement.* This paper was edited by and reviewed by.

586

587 **References**

588 Alves, B. J. R., Smith, K. A., Flores, R. A., Cardoso, A. S., Oliveira, W. R. D., Jantalia,

589 C. P., Urquiaga, S., and Boddey, R. M.: Selection of the most suitable sampling

590 time for static chambers for the estimation of daily mean N₂O flux from soils,

591 Soil Biol Biochem, 46, 129-135, <https://doi.org/10.1016/j.soilbio.2011.11.022>,

592 2012.

593 Brooks, P. D., Schmidt, S. K., and Williams, M. W.: Winter production of CO₂ and

594 N₂O from alpine tundra: environmental controls and relationship to inter-system

595 C and N fluxes, Oecologia, 110, 403-413, <https://doi.org/10.1007/pl00008814>,

596 1997.

597 Castaldi, S., Bertolini, T., Valente, A., Chiti, T., and Valentini, R.: Nitrous oxide

598 emissions from soil of an African rain forest in Ghana, Biogeosciences, 10,

599 4179-4187, <https://doi.org/10.5194/bg-10-4179-2013>, 2013.

600 Chantigny, M. H., Rochette, P., Angers, D. A., Goyer, C., Brin, L. D., and Bertrand, N.:

601 Nongrowing season N₂O and CO₂ emissions - Temporal dynamics and influence

602 of soil texture and fall-applied manure, Can J Soil Sci, 97, 452-464,

603 <https://doi.org/10.1139/cjss-2016-0110>, 2017.



- 604 Chen, X. P., Wang, G. X., Zhang, T., Mao, T. X., Wei, D., Hu, Z. Y., and Song, C. L.:
605 Effects of warming and nitrogen fertilization on GHG flux in the permafrost
606 region of an alpine meadow, *Atmos Environ*, 157, 111-124,
607 <https://doi.org/10.1016/j.atmosenv.2017.03.024>, 2017.
- 608 Cui, Q., Song, C. C., Wang, X. W., Shi, F. X., Yu, X. Y., and Tan, W. W.: Effects of
609 warming on N₂O fluxes in a boreal peatland of permafrost region, Northeast
610 China, *Sci Total Environ*, 616-617, 427-434,
611 <https://doi.org/10.1016/j.scitotenv.2017.10.246>, 2018.
- 612 Dietzel, R., Wolfe, D., and Thies, J. E.: The influence of winter soil cover on spring
613 nitrous oxide emissions from an agricultural soil, *Soil Biol Biochem*, 43,
614 1989-1991, <https://doi.org/10.1016/j.soilbio.2011.05.017>, 2011.
- 615 Ding, W. X., Cai, Y., Cai, Z. C., Yagi, K., and Zheng, X. H.: Nitrous oxide emissions
616 from an intensively cultivated maize-wheat rotation soil in the North China Plain,
617 *Sci Total Environ*, 373, 501-511, <https://doi.org/10.1016/j.scitotenv.2006.12.026>,
618 2007.
- 619 Dobbie, K. E., and Smith, K. A.: The effect of water table depth on emissions of N₂O
620 from a grassland soil, *Soil Use and Management*, 22, 22-28,
621 <https://10.1111/j.1475-2743.2006.00002.x>, 2006.
- 622 Du, R., Lu, D. R., and Wang, G. C.: Diurnal, seasonal, and inter-annual variations of
623 N₂O fluxes from native semi-arid grassland soils of inner Mongolia, *Soil Biology
624 & Biochemistry*, 38, 3474-3482, <https://10.1016/j.soilbio.2006.06.012>, 2006.
- 625 Dunmola, A. S., Tenuta, M., Moulin, A. P., Yapa, P., and Lobb, D. A.: Pattern of



626 greenhouse gas emission from a Prairie Pothole agricultural landscape in
627 Manitoba, Canada, *Can J Soil Sci*, 90, 243-256, <https://doi.org/10.4141/cjss08053>,
628 2010.

629 Flesch, T. K., Baron, V. S., Wilson, J. D., Basarab, J. A., Desjardins, R. L., Worth, D.,
630 and Lemke, R. L.: Micrometeorological measurements reveal large nitrous oxide
631 losses during spring thaw in Alberta, *Atmosphere*, 9, 128,
632 <https://doi.org/10.3390/atmos9040128>, 2018.

633 Fu, Y., Liu, C., Lin, F., Hu, X., Zheng, X., Zhang, W., and Ca, G.: Quantification of
634 year-round methane and nitrous oxide fluxes in a typical alpine shrub meadow on
635 the Qinghai-Tibetan Plateau, *Agr Ecosyst Environ*, 255, 27-36,
636 <https://doi.org/10.1016/j.agee.2017.12.003>, 2018.

637 Furon, A. C., Wagner-Riddle, C., Smith, C. R., and Warland, J. S.: WaveRet analysis
638 of wintertime and spring thaw CO₂ and N₂O fluxes from agricultural fields, *Agric
639 For Meteorol*, 148, 1305-1317, <https://doi.org/10.1016/j.agrformet.2008.03.006>,
640 2008.

641 Gao, W. F., Yao, Y. L., Gao, D. W., Wang, H., Song, L. Q., Sheng, H. C., Cai, T. J.,
642 and Liang, H.: Responses of N₂O emissions to spring thaw period in a typical
643 continuous permafrost region of the Daxing'an Mountains, northeast China,
644 *Atmos Environ*, 214, 116822, <https://doi.org/10.1016/j.atmosenv.2019.116822>,
645 2019a.

646 Gao, W. F., Yao, Y. L., Liang, H., Song, L. Q., Sheng, H. C., Cai, T. J., and Gao, D. W.:
647 Emissions of nitrous oxide from continuous permafrost region in the Daxing'an



- 648 Mountains, Northeast China, Atmos Environ, 198, 34-45,
649 <https://doi.org/10.1016/j.atmosenv.2018.10.045>, 2019b.
- 650 Gil, J., Pérez, T., Boering, K., Martikainen, P. J., and Biasi, C.: Mechanisms
651 responsible for high N₂O emissions from subarctic permafrost peatlands studied
652 via stable isotope techniques, Global Biogeochem Cy, 31, 172-189,
653 <https://doi.org/10.1002/2015GB005370>, 2017.
- 654 Glenn, A. J., Tenuta, M., Amiro, B. D., Maas, S. E., and Wagner-Riddle, C.: Nitrous
655 oxide emissions from an annual crop rotation on poorly drained soil on the
656 Canadian Prairies, Agricultural and Forest Meteorology, 166, 41-49,
657 <https://10.1016/j.agrformet.2012.06.015>, 2012.
- 658 Hao, Q. J., Wang, Y. S., Song, C. C., and Huang, Y.: Contribution of winter fluxes to
659 the annual CH₄, CO₂ and N₂O emissions from freshwater marshes in the Sanjiang
660 Plain, J Environ Sci-China, 18, 270-275,
661 <https://doi.org/10.3321/j.issn:1001-0742.2006.02.012> 2006.
- 662 Harden, J. W., Koven, C. D., Ping, C. L., Hugelius, G., David McGuire, A., Camill, P.,
663 Jorgenson, T., Kuhry, P., Michaelson, G. J., O'Donnell, J. A., Schuur, E. A. G.,
664 Tarnocai, C., Johnson, K., and Grosse, G.: Field information links permafrost
665 carbon to physical vulnerabilities of thawing, Geophys Res Lett, 39, L15704,
666 <https://doi.org/10.1029/2012GL051958>, 2012.
- 667 Hou, H., Peng, S., Xu, J., Yang, S., and Mao, Z.: Seasonal variations of CH₄ and N₂O
668 emissions in response to water management of paddy fields located in Southeast
669 China, Chemosphere, 89, 884-892, <https://10.1016/j.chemosphere.2012.04.066>,



670 2012.

671 Hutchinson, G. L., Livingston, G. P., Healy, R. W., and Striegl, R. G.: Chamber
672 measurement of surface-atmosphere trace gas exchange: numerical evaluation of
673 dependence on soil, interfacial layer, and source/sink properties, *J Geophys*
674 *Res-Atmos*, 105, 8865-8875, <https://doi.org/10.1029/1999JD901204>, 2000.

675 IPCC: Climate change 2013: The physical science basis: Working group I
676 contribution to the fifth assessment report of the Intergovernmental Panel on
677 Climate Change, Cambridge, UK, and New York, USA, Cambridge University
678 Press, 2013.

679 Jin, H. J., Yu, Q. H., Lii, L. Z., Guo, D. X., He, R. X., Yu, S. P., Sun, G. Y., and Li, Y.
680 W.: Degradation of permafrost in the Xing'anling Mountains, northeastern China,
681 *Permafrost Periglac*, 18, 245-258, <https://doi.org/10.1002/ppp.589>, 2007.

682 Lamb, E. G., Han, S., Lanoil, B. D., Henry, G. H. R., Brummell, M. E., Banerjee, S.,
683 and Siciliano, S. D.: A High Arctic soil ecosystem resists long-term
684 environmental manipulations, *Global Change Biol*, 17, 3187-3194,
685 <https://doi.org/10.1111/j.1365-2486.2011.02431.x>, 2011.

686 Li, K. H., Gong, Y. M., Song, W., Lv, J. L., Chang, Y. H., Hu, Y. K., Tian, C. Y.,
687 Christie, P., and Liu, X. J.: No significant nitrous oxide emissions during spring
688 thaw under grazing and nitrogen addition in an alpine grassland, *Global Change*
689 *Biol*, 18, 2546-2554, <https://doi.org/10.1111/j.1365-2486.2012.02704.x>, 2012.

690 Liu, F. Q., Zhang, Y. P., Liang, H., and Gao, D. W.: Long-term harvesting of reeds
691 affects greenhouse gas emissions and microbial functional genes in alkaline



- 692 wetlands, *Water Res*, 164, 114936, <https://doi.org/10.1016/j.watres.2019.114936>,
- 693 2019.
- 694 Ma, W. K., Schautz, A., Fishback, L. A. E., Bedard-Haughn, A., Farrell, R. E., and
- 695 Siciliano, S. D.: Assessing the potential of ammonia oxidizing bacteria to produce
- 696 nitrous oxide in soils of a high arctic lowland ecosystem on Devon Island,
- 697 Canada, *Soil Biol Biochem*, 39, 2001-2013,
- 698 <https://doi.org/10.1016/j.soilbio.2007.03.001>, 2007.
- 699 Maljanen, M., Alm, J., Martikainen, P. J., and Repo, T.: Prolongation of soil frost
- 700 resulting from reduced snow cover increases nitrous oxide emissions from boreal
- 701 forest soil, *Boreal Environ Res*, 15, 34-42, 2010.
- 702 Marushchak, M. E., Pitkamaki, A., Koponen, H., Biasi, C., Seppala, M., and
- 703 Martikainen, P. J.: Hot spots for nitrous oxide emissions found in different types
- 704 of permafrost peatlands, *Global Change Biol*, 17, 2601-2614,
- 705 <https://doi.org/10.1111/j.1365-2486.2011.02442.x>, 2011.
- 706 Merbold, L., Steinlin, C., and Hagedorn, F.: Winter greenhouse gas fluxes (CO₂, CH₄
- 707 and N₂O) from a subalpine grassland, *Biogeosciences*, 10, 3185-3203,
- 708 <https://10.5194/bg-10-3185-2013>, 2013.
- 709 Mu, C. C., Abbott, B. W., Zhao, Q., Su, H., Wang, S. F., Wu, Q. B., Zhang, T. J., and
- 710 Wu, X. D.: Permafrost collapse shifts alpine tundra to a carbon source but
- 711 reduces N₂O and CH₄ release on the northern Qinghai-Tibetan Plateau, *Geophys*
- 712 *Res Lett*, 44, 8945-8952, <https://doi.org/10.1002/2017GL074338>, 2017.
- 713 Oquist, M. G., Nilsson, M., Sorensson, F., Kasimir-Klemedtsson, A., Persson, T.,



- 714 Weslien, P., and Klemetsson, L.: Nitrous oxide production in a forest soil at low
715 temperatures - processes and environmental controls, *Fems Microbiol Ecol*, 49,
716 371-378, <https://doi.org/10.1016/j.femsec.2004.04.006>, 2004.
- 717 Paré, M. C., and Bedard-Haughn, A.: Landscape-scale N mineralization and
718 greenhouse gas emissions in Canadian Cryosols, *Geoderma*, 189, 469-479,
719 <https://doi.org/10.1016/j.geoderma.2012.06.002>, 2012.
- 720 Repo, M. E., Susiluoto, S., Lind, S. E., Jokinen, S., Elsakov, V., Biasi, C., Virtanen, T.,
721 and Martikainen, P. J.: Large N₂O emissions from cryoturbated peat soil in tundra,
722 *Nat Geosci*, 2, 189-192, <https://doi.org/10.1038/NGEO434>, 2009.
- 723 Siljanen, H., J.E. Alves, R., Ronkainen Jussi, G., Lamprecht, R., Bhattarai, H. R.,
724 Bagnoud, A., Marushchak, M., Martikainen, P., Schleper, C., and Biasi, C.:
725 Archaeal nitrification is a key driver of high nitrous oxide emissions from arctic
726 peatlands, *Soil Biol Biochem*, 137, 107539,
727 <https://doi.org/10.1016/j.soilbio.2019.107539>, 2019.
- 728 Song, C. C., Zhang, J. B., Wang, Y. Y., Wang, Y. S., and Zhao, Z. C.: Emission of CO₂,
729 CH₄ and N₂O from freshwater marsh in northeast of China, *J Environ Manage*,
730 88, 428-436, <https://doi.org/10.1016/j.jenvman.2007.03.030>, 2008.
- 731 Takakai, F., Desyatkin, A. R., Lopez, C. M. L., Fedorov, A. N., Desyatkin, R. V., and
732 Hatano, R.: CH₄ and N₂O emissions from a forest-alas ecosystem in the
733 permafrost taiga forest region, eastern Siberia, Russia, *J Geophys Res-Biogeosci*,
734 113, G02002, <https://doi.org/10.1029/2007JG000521>, 2008.
- 735 Tatti, E., Goyer, C., Chantigny, M., Wertz, S., Zebarth, B. J., Burton, D. L., and Filion,



- 736 M.: Influences of over winter conditions on denitrification and nitrous
737 oxide-producing microorganism abundance and structure in an agricultural soil
738 amended with different nitrogen sources, *Agr Ecosyst Environ*, 183, 47-59,
739 <https://doi.org/10.1016/j.agee.2013.10.021>, 2014.
- 740 Virkajärvi, P., Maljanen, M., Saarijärvi, K., Haapala, J., and Martikainen, P. J.: N₂O
741 emissions from boreal grass and grass - clover pasture soils, *Agr Ecosyst Environ*,
742 137, 59-67, <https://doi.org/10.1016/j.agee.2009.12.015> 2010.
- 743 Voigt, C., Lamprecht, R. E., Marushchak, M. E., Lind, S. E., Novakovskiy, A., Aurela,
744 M., Martikainen, P. J., and Biasi, C.: Warming of subarctic tundra increases
745 emissions of all three important greenhouse gases – carbon dioxide, methane, and
746 nitrous oxide, *Global Change Biol*, 23, 3121-3138,
747 <https://doi.org/10.1111/gcb.13563>, 2017.
- 748 Wertz, S., Goyer, C., Zebarth, B. J., Burton, D. L., Tatti, E., Chantigny, M. H., and
749 Filion, M.: Effects of temperatures near the freezing point on N₂O emissions,
750 denitrification and on the abundance and structure of nitrifying and denitrifying
751 soil communities, *Fems Microbiol Ecol*, 83, 242-254,
752 <https://doi.org/10.1111/j.1574-6941.2012.01468.x>, 2013.
- 753 Wu, X., Brueggemann, N., Gasche, R., Shen, Z. Y., Wolf, B., and Butterbach-Bahl, K.:
754 Environmental controls over soil-atmosphere exchange of N₂O, NO, and CO₂ in
755 a temperate Norway spruce forest, *Global Biogeochem Cy*, 24, GB2012,
756 <https://doi.org/10.1029/2009GB003616>, 2010.
- 757 Wu, X. W., Ma, D. L., Ren, J. H., Chen, Q., and Dong, X. F.: Emissions of CO₂, CH₄,



758 and N₂O Fluxes from forest soil in permafrost region of Daxing'an Mountains,
759 northeast China, Int J Env Res Pub He, 16, 2999,
760 <https://doi.org/10.3390/ijerph16162999>, 2019.

761 Yanai, Y., Hirota, T., Iwata, Y., Nemoto, M., Nagata, O., and Koga, N.: Accumulation
762 of nitrous oxide and depletion of oxygen in seasonally frozen soils in northern
763 Japan - Snow cover manipulation experiments, Soil Biol Biochem, 43,
764 1779-1786, <https://doi.org/10.1016/j.soilbio.2010.06.009>, 2011.

765 Zhang, H., Yao, Z. S., Wang, K., Zheng, X. H., Ma, L., Wang, R., Liu, C. Y., Zhang,
766 W., Zhu, B., Tang, X. Y., Hu, Z. H., and Han, S. H.: Annual N₂O emissions from
767 conventionally grazed typical alpine grass meadows in the eastern
768 Qinghai-Tibetan Plateau, Sci Total Environ, 625, 885-899,
769 <https://doi.org/10.1016/j.scitotenv.2017.12.216>, 2018.

770